INTERACTION OF POLYVINYLTHIOL-FUNCTIONALIZED SILVER NANOPARTICLES WITH BOVINE SERUM ALBUMIN

M. SAJID ALI[a*], H. A. AL-LOHEDAN[a], M. SHAMSUL OLA[b], A. M. ATTA[a]
[a]*Surfactant Research Chair, Department of Chemistry, King Saud University, P.O. Box-2455, Riyadh - 11451, Saudi Arabia*
[b]*Department of Biochemistry, King Saud University, P.O. Box-2455, Riyadh - 11451, Saudi Arabia*

Biomacromolecule-nanoparticle interaction is an important tool for controlling several cellular and extracellular processes. Nanoparticles, when introduces in any biological fluids, have likelihoods to interact with biomolecules, particularly, with proteins and nucleic acids. In this study, silver nanoparticles were functionalized with polyvinylthiol (Ag-PVT) and characterized by TEM. Absorbance, intrinsic, extrinsic & synchronous fluorescence, and circular dichroism measurements were performed to understand the conjugation of bovine serum albumin (BSA) and Ag-PVT nanoparticles. Quenching of BSA fluorescence by Ag-PVT nanoparticles was a result of the formation of BSA-nanoparticle complex by a static mechanism. A significant change on secondary structure of BSA was confirmed with both CD and synchronous fluorescence results. Fluorescence quenching results were analyzed by using Stern-Volmer equation. Ag-PVT nanoparticles were found to be bounded by hydrophobic patches of BSA and displaced the hydrophobic external probe 1-anilino-8-naphthalene-sulfonate (ANS). By using Förster resonance energy transfer (FRET) it was found that Ag-PVT is located in the close proximity of the BSA.

1. Introduction

The demand of the nanotechnology is mounting progressively with a stimulating rising in the field of nanomaterials and biomolecules interactions [1, 2]. A range of intriguing characteristics such as size compatibility to biomolecules, high surface to volume ratio, biomimetic functionalization, etc., are responsible for their extensive applications in biotechnology, pharmaceutical and medical fields [3−5]. Silver nanoparticles (AgNPs) are well known to possess a variety of special properties of which the most important are antimicrobial, catalytic and enhanced optical properties [6] while others include applications in alveolar bone surgery [7], in dental practices as restorative material, endodontic retrofill cements, and dental implants [8]. These are even effective to kill the microbes which are multi-drug resistant [9].

Though, nanoparticles retain exceptional physical and chemical properties they, generally, lack apposite surface properties for particular applications [10]. The coating or functionalization of nanoparticles greatly affects their stability, function and toxicity, particularly, for biomedical applications [11]. Functionalization of nanoparticles is necessary to meet some requirements, for their efficient clinical use, such as good dispersibility and stability unaffected by cellular environment, high selectivity for tissue targeting, limited non-specific binding with albumins and low renal toxicity [12].

---

*Corresponding author: smsajidali@gmail.com

AgNPs have also been surface functionalized with various groups such as, silica [13], poly(ethylenimine) [14], thiosalicylic acid [15], phospholipids [16], etc. Several attempts have also been made to modify the surfaces of AgNPs with thiol groups [17-23]. Recently, we have modified the surface of AgNPs by functionalizing these with polyvinylthiol [24] and in present investigation we have seen effect of these nanoparticles on the conformation of the bovine serum albumin (BSA).

Serum albumins, the most abundant proteins in circulatory system which constitute around 60% of total plasma protein, are accountable for the transport, distribution and metabolism of many endogenous and exogenous ligands e.g., fatty acids, amino acids and drugs. These are also responsible for maintaining the osmotic pressure and pH of blood. Bovine serum albumin is among one of the most studied proteins and shows 76% similarity with that of human serum albumin [25]. BSA is alpha helical protein with 67% helical content and consisting of 583 amino acids. It is divided into three structurally similar domains (I, II, and III) each of which is further divided into two sub domains (A and B) [26]. Binding of nanoparticles with serum albumins has been studied in order to get insight on the possible applications of nanoparticles in drug delivery [27-32]. Since both nanoparticles and albumins play important roles in drug delivery systems and will be in close proximity when drug-loaded nanoparticles be administrated. It will be the binding efficiency of the drug with nanoparticles which will affect the transport of the drug in the circulatory system. Nanoparticles may also affect the conformation of albumins, which may, eventually, affect the transport properties of the albumins. Therefore, understanding the interaction of albumins with nanoparticles is necessary. Thiol capped AgNPs have been found to possess good optical and physical properties and can be used in various applications including drug formulations [17-23].

In this work, we are reporting binding of polyvinylthiol-capped nanoparticles (Ag-PVT) with BSA by means of optical, fluorescence (Intrinsic, extrinsic and synchronous) and circular dichroism spectroscopies.

2. Experimental

2.1 Materials

BSA (lyophilized powder, Fatty acid free, Globulin free, ≥99%, Sigma) silver nitrate (ACS reagent, ≥98.0%, Sigma) and poly (vinyl alcohol) (PVA, molecular weight 80,000 g mol^{-1} and 88% degree of hydrolysis, Aldrich) were used without further purification. Rest of the chemicals/reagents used in the study were of analytical grade and purchased from Sigma, USA and used as received. Poly (vinyl thiol) (PVA-SH) was prepared in the laboratory by the methods described elsewhere taking PVA as starting material [24]. Ag-PVT nanoparticles were synthesized by adding PVA-SH with silver nitrate solution. The details related to the Ag-PVT nanoparticles synthesis and characterizations are given in our previous publication [24, 33].

2.2 Sample preparation

A stock solution of BSA was made in 20 mM of pH 7.4 tris HCl buffer and protein concentration of 2 μM was used throughout. Tris-HCl buffer was filtered through a 0.45 μm Millipore Millex-HV PVDF filter and pH was measured by using Mettler-Toledo pH meter (model S20).

2.3 UV–Vis absorption measurements

UV–Vis spectra were performed with Perkin-Elmer Lambda 650 Spectrophotometer equipped with autosampler and water-bath with temperature controller in the wavelength range of 240 - 320 nm. Quartz cuvettes of 1 cm path length were used for the measurements.

2.4 Fluorescence measurements

Fluorescence measurements were performed on Hitachi spectrofluorometer (Model F 7000) equipped with a PC and programmable temperature controller. The fluorescence spectra were collected at 25 °C with a path length cell of 1 cm. The excitation and emission slits were set at 5 nm. Intrinsic fluorescence was measured by exciting BSA at 295 nm which is the excitation peak for the tryptophan residue. The decrease in fluorescence intensity at particular wavelength was analyzed according to the Stern–Volmer equation [34]:

$$\frac{F_o}{F} = K_{sv} [Q] + 1 \tag{1}$$

where F_o and F are the fluorescence intensities in absence and presence of quencher (Ag-PVT), K_{sv} is the Stern-Volmer quenching constant and:

$$K_{sv} = k_q \tau_0 \tag{2}$$

where k_q is the bimolecular rate constant of the quenching reaction and τ_o the average integral fluorescence life time of Trp which is $\sim 5.7 \times 10^{-9}$ sec. [35]. Binding constants and binding sites were obtained from [36]:

$$\log\left(\frac{F_o}{F} - 1\right) = \log K_b + n \log [Q] \tag{3}$$

where, K_b is the binding constant and n is number of binding sites.
  The free energy of binding can be defined as:

$$\Delta G^o = -RT \ln K_b \tag{4}$$

where R is the gas constant (1.987 J K^{-1}mol^{-1}) and T is the temperature in Kelwin.
  For extrinsic fluorescence measurements in the ANS binding studies, the excitation was set at 380 nm, and the emission spectra were taken in the range of 400−600 nm. Concentration of ANS used in this study was 100 µM. Synchronous fluorescence spectra were collected at $\Delta\lambda = 15$ nm and $\Delta\lambda = 60$ nm which are characteristics for the tyrosine and tryptophan residues, respectively. Resonance Rayleigh scattering was performed by simultaneous excitation and emission at 350 nm and both excitation and emission slits were set at 5 nm.

2.5 Circular Dichroism measurement

The circular dichroism studies of BSA in presence of Ag-PVT were carried out with JASCO J-815 spectropolarimeter equipped with a Peltier-type temperature controller. The instrument was calibrated with d-10-camphorsulfonic acid [37]. All the CD spectra were collected in a cell of 0.5 mm path-length. The scan speed was 100 nm/min and response time of 1 s for all measurements. Each spectrum was the average of 2 scans. The raw data obtain in millidegrees were converted to mean residue ellipticity (MRE) in degcm^2 dmol^{-1}, which is given by:

$$MRE = \frac{\theta_{obs}(m\deg)}{10 \times n \times C \times l} \tag{5}$$

where θ_{obs} is the observed ellipticity in millidegrees, C is the concentration of protein in molar, n is the number of amino acid residues and l is the length of the light path in centimeter. All spectra were smoothed by the Savitzky–Golay method with 10 convolution width. Alpha helical content

was calculated from the MRE values at 222 nm using the following equation as described by Chen *et al*. [38] and also cross checked by K2D software [39]:

$$\%\alpha\text{-helix} = \left(\frac{MRE_{222\,nm} - 2{,}340}{30{,}300} \right) \times 100 \tag{6}$$

3. Results and discussions

UV-visible spectra of BSA in the absence and presence of various Ag-PVT NPs concentrations are given in Fig. 1. The absorption peak around 280 nm is due to the absorption of tryptophan, tyrosine and phenyl alanine. It could be observed from the figure that absorption intensity of BSA increased with addition of Ag-PVT nanoparticles [33, 40, 41] this is a clear indication of the interaction between Ag-PVT nanoparticles and BSA.
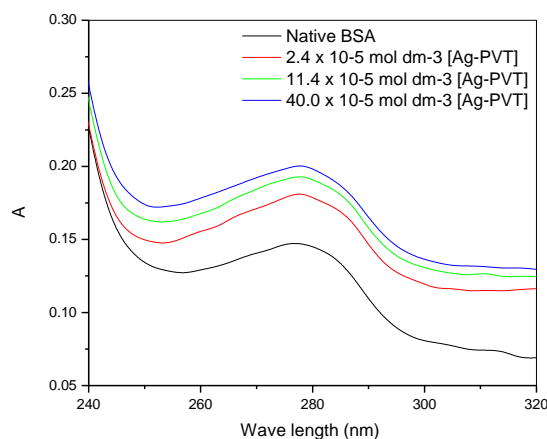

Fig. 1. UV-Visible spectra of BSA in absence and presence of Ag-PVT nanoparticles.
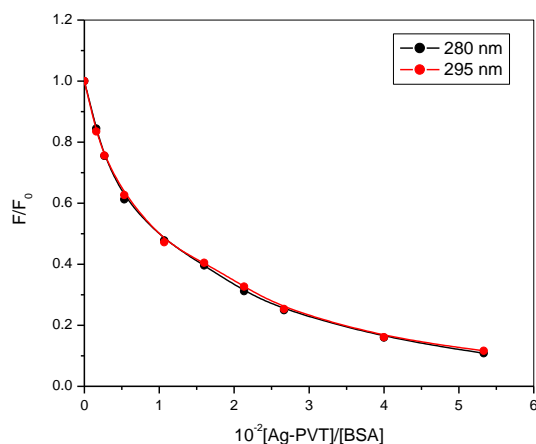

Fig. 2. A comparison of the extent of fluorescence quenching of BSA in presence of Ag-PVT at excitation wavelengths of 280 and 295 nm.

BSA owns two tryptophan (Trp) residues Trp213, located within a highly hydrophobic binding pocket of the protein (site-I), and Trp134, located on the surface of the molecule (site-II) [26] while 20 tyrosine residues are distributed along the whole polypeptide domain. When protein is excited at 280 nm the fluorescence mainly comes from tryptophan and partly from tyrosine due

to efficient resonance energy transfer from tyrosine to tryptophan [42]. Whereas upon excitation at 295 the fluorescence emission is typically comes from the tryptophan residues. Figure 2 illustrates the plots of F/F_0 versus [Ag- PVT]/[BSA] at both excitation wavelengths, where F_0 and F are
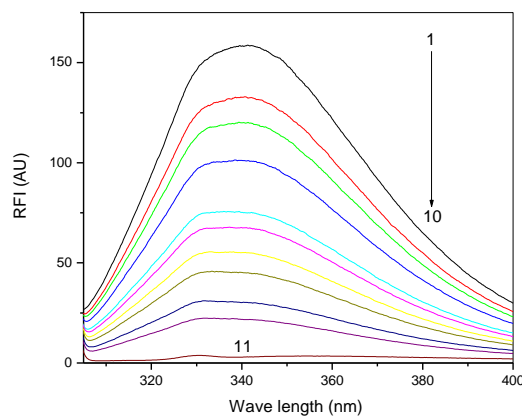

Fig. 3. Fluorescence emission spectra of BSA in absence and presence of Ag-PVT nanoparticles; [BSA] = 1.5 x 10^{-6} mol dm^{-3}, [Ag-PVT] = 0, 2.4, 4, 8, 16, 24, 32, 40, 60, 80 x 10^{-5} mol dm^{-3} (curves 1-10) curve 11 is 80 x 10^{-5} mol dm^{-3} pure Ag-PVT (λ_{ex}=295nm).

the fluorescence intensities before and after the addition of nanoparticles, respectively. Since there was no change in the observed quenching of BSA at these wavelengths, it can be concluded that only tryptophan is responsible for the fluorescence quenching of BSA by nanoparticles with negligible contribution from tyrosine. Therefore, we have selected only 295 nm as excitation wavelengths for our further studies.

The effect of Ag-PVT nanoparticles on the quenching of BSA at 25 °C and pH 7.4 has been given in Fig. 3. It was observed from the figure that fluorescence intensity gradually decreased on increasing the Ag-PVT nanoparticles concentration while the peak position showed a significant blue shift from 340 to 332 nm. It is, therefore, concluded that BSA and Ag-PVT interacted with each other which induced the microenvironment around BSA and the blue shift was a result of the increased hydrophobicity around the fluorescent chromophores of BSA after the addition of Ag-PVT nanoparticles [43].

The fluorescence quenching usually takes place by two mechanisms, dynamic and static, which depend on the way of interaction between quencher and albumin [33]. Dynamic quenching occurs when quencher molecules have enough energy to collide with the excited state fluorophore of albumin to bring it to the ground state. In contrast, the formation of non-fluorescent ground state complex between quencher and fluorophore gives rise to the static quenching. The Stern–Volmer plots of the quenching of BSA fluorescence by Ag-PVT nanoparticles are given in Fig. 4. The data were fitted according to Eq. 1 and there was a linear dependence between F_0/F versus [Ag-PVT]. The calculated K_{SV} and k_q values were found to be 7.22 x 10^3 L mol^{-1} and 1.27 x 10^{12} L mol^{-1} s^{-1}, respectively. The maximum scatter collision quenching constant of various quenchers with biopolymer is 2.0×10^{10} L mol^{−1} s^{−1} [44]. The rate constant of quenching for Ag-PVT was greater than the maximum value of k_q for the scatter mechanism. This is an indication of the involvement of static quenching between them [40].
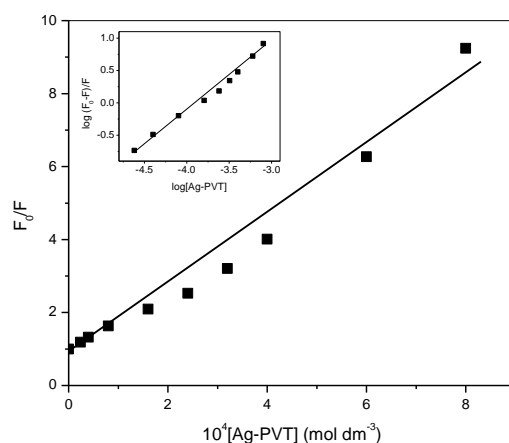
Fig. 4. Stern-Volmer plots for the quenching of BSA by Ag-PVT nanoparticles at 25 °C. Inset: Plot of log (F_0–F)/F as a function of log [Ag-PVT].

The inset of Fig. 4 shows the plot of log (F_0–F)/F versus log [Ag-PVT] which is used to calculate the binding parameters involved in BSA and Ag-PVT nanoparticles interaction (Eq. 3). The value of binding constant is significant to understand the distribution of the drug in plasma since the weak binding can lead to a short lifetime or poor distribution, while strong binding can decrease the concentration of free drug in plasma. The binding constant, K_b, was found to be 4.45 x 10^3 L mol^{-1} and the number of binding site for Ag-PVT nanoparticles to the BSA was found to be one with free energy of binding, ΔG^0, equal to 21.66 kJ mol^{-1}.

8-anilinonaphthalene-1-sulfonate (ANS) is a hydrophobic dye extensively exploited for probing the nonpolar character of proteins, membranes, and other microheterogeneous systems [44]. In general the dye binds to the less polar hydrophobic environment of proteins with subsequent blue shift of the emission maximum with an increase in emission intensity. Free ANS shows feeble fluorescence intensity with λ_{max} at 526 nm while in presence of native BSA fluorescence intensity of ANS increased by several times with blue shift at 472 nm (Fig. 5). This shows strong binding between the albumin and dye. Addition of the Ag-PVT nanoparticles to the BSA-ANS system causes the decrease in the fluorescence intensity of the dye with a significant red-shift of the absorption maximum. The interaction between the Ag-PVT nanoparticles and albumin probably resulted in the weakening of the ANS–BSA binding with an associated conformational change of the protein in order to accommodate the silver nanoparticle [45].
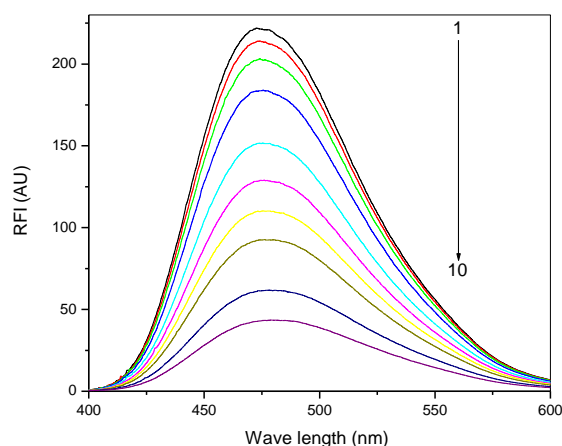

Fig. 5. Effect of [Ag-PVT] on the ANS fluorescence emission spectra. [BSA] = 1.5 x 10^{-6} mol dm^{-3}, [Ag-PVT] = 0, 2.4, 4, 8, 16, 24, 32, 40, 60, 80 x 10^{-5} mol dm^{-3} (λ_{ex} = 380 nm & [ANS] = 100 x 10^{-6} mol dm^{-3}).

Synchronous fluorescence spectroscopy is a common method for evaluating the conformational changes of the protein. This is a useful method to study the molecular environment in the vicinity of the fluorophore. While maintaining the sensitivity associated with fluorescence, synchronous spectra offer several advantages such as spectral simplification, spectral bandwidth reduction, and the avoidance of different perturbing effects [46]. The synchronous spectra are a characteristic of the typical Trp residue fluorescence at $\Delta\lambda$ (λ_{em}- λ_{ex}) = 60 nm, while they are characteristic of the typical Tyr residue fluorescence at $\Delta\lambda$ = 15 nm. Effect of Ag-PVT nanoparticles on the synchronous fluorescence spectra of BSA is given in Fig. 6 (a) and (b). As the concentration of Ag-PVT increases intensity of the BSA fluorescence decreases with a substantial blue shift in its λ_{max}. This is a clear indication of the alteration of the hydrophobicity surrounding Trp and Tyr residues. The observed blue shift indicates that hydrophobicity around these residues (Trp and Tyr) is increasing and this may be probably due to the interaction between polyvinythiol coating of silver nanoparticles with hydrophobic patches of BSA.
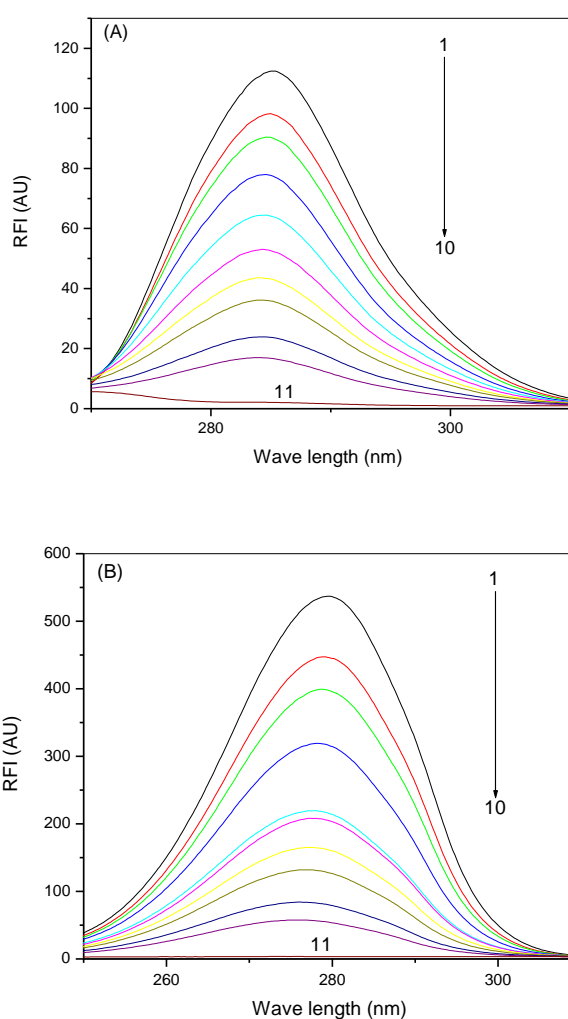

Fig. 6. Synchronous fluorescence spectra of interaction of BSA with Ag-PVT nanoparticles (A) $\Delta\lambda$ = 15 (B) $\Delta\lambda$ = 60. [BSA] = 1.5 x 10^{-6} mol dm^{-3}, [Ag-PVT] = 0, 2.4, 4, 8, 16, 24, 32, 40, 60, 80 x 10^{-5} mol dm^{-3} (curves 1-10) curve 11 is 80 x 10^{-5} mol dm^{-3} pure Ag-PVT.

Influence of the Ag-PVT nanoparticles on the secondary structures conformations of BSA was investigated by employing CD spectropolarimetry. BSA falls under the category of α-helical proteins which contains around 67% of α-helical content [47]. Interaction of BSA with solvent or any other substance may give rise to the changes in its secondary structure or α-helical contents.

The far-UV wavelength range of CD spectra (generally ranges from ~200 to 250 nm) can provide information on the polypeptide backbone conformation of proteins. CD is proficient of finding information for practically all secondary structural variants, such as α-helices, β-sheets, β-turns, and random coil structures. All of these structures provide origins to bands of distinct forms and degrees in the far-UV region. α-helices show large CD absorption with negative ellipticity at 222 and 208 nm and positive ellipticity at 193 nm [48,49].
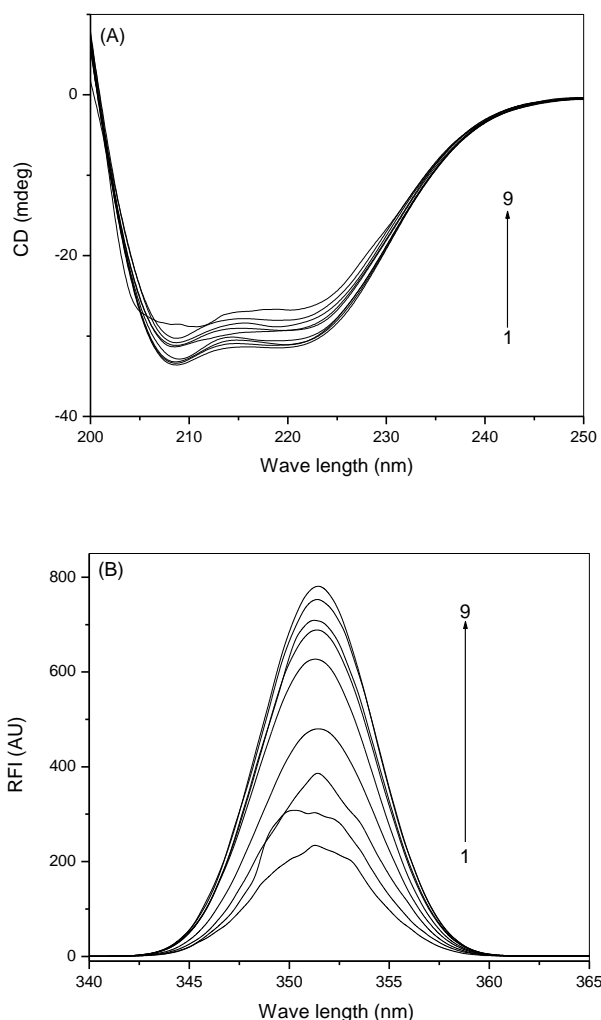

Fig. 7. (A) Far-UV CD spectra of interaction of BSA with Ag-PVT nanoparticles. (B) Resonance Rayleigh scattering plots with [Ag-PVT] = 0, 2.4, 4, 8, 16, 32, 40, 60, 80 x 10^{-5} mol dm^{-3} and [BSA] = 1.5 x 10^{-6} mol dm^{-3}.

Modifications of ellipticity at 222 nm (−MRE222) are convenient methods for observing changes in α-helical content. Several CD spectra in presence and absence of various concentrations of Ag-PVT are given in Fig. 7 (A). Equations 5 and 6 have been used to calculate the α-helicity of the BSA in presence of various amounts of Ag-PVT nanoparticles and the results are presented in Table 1. From the quantitative analysis it was found that α-helical content of the native BSA was found to be 66.08 % which was in good agreement of the literature value. However, a considerable reduction in the α-helix from 66.06% to 54.85% for the concentrations of Ag-PVT nanoparticles ranging from 2.4 to 80 x 10^{-5} mol dm^{-3} was observed, which was indicative of the loss of the α-helix as a results of the interaction between albumin and nanoparticles. Therefore, it is inferred that the binding of Ag-PVT to BSA induced the conformational changes in BSA with partial unfolding of the biomacromolecule.

Table 1. Secondary structure analysis from the native BSA and BSA–Ag-PVT complexes at pH 7.4 and 25 °C.

10^5[Ag-PVT] (mol dm^{-3})	% α-helix
0	66.08
2.4	65.49
4	64.63
8	62.51
16	60.86
24	59.83
40	57.63
60	55.46
80	54.85

Rayleigh scattering was also performed to see the effect of the Ag-PVT nanoparticles on the aggregation behavior of BSA [41]. RRS is important tool and has been widely applied to the determination of biological macromolecules. Effect of Ag-PVT nanoparticles on the RRS of the BSA was such that when the concentration of the nanoparticles increased intensity gradually increased and reaches upto about 4 times under our experimental conditions. This is a clear indication of the unfolding of BSA by Ag-PVT nanoparticles, though, partial as indicated by CD analyses (Fig. 7 B). [50, 51].

Förster resonance energy transfer (FRET) is a distance dependent interaction in which transfer of excitation energy takes place form donor to acceptor, nonradiatively. We have also observed the spectral overlap between the fluorescence emission spectra of free BSA and absorption spectrum of Ag-PVT nanoparticles (Fig. 8). According FRET theory [52] energy transfer is likely to happen under the following conditions: (i) the relative orientation of the donor and acceptor dipoles, (ii) the extent of overlap of fluorescence emission spectrum of the donor with the absorption spectrum of the acceptor, and (iii) the distance between the donor and the acceptor is less than 8 nm. Based on Förster's theory, the efficiency of energy transfer (E) is related to the distance r between donor and acceptor by Eq. (7) [53].
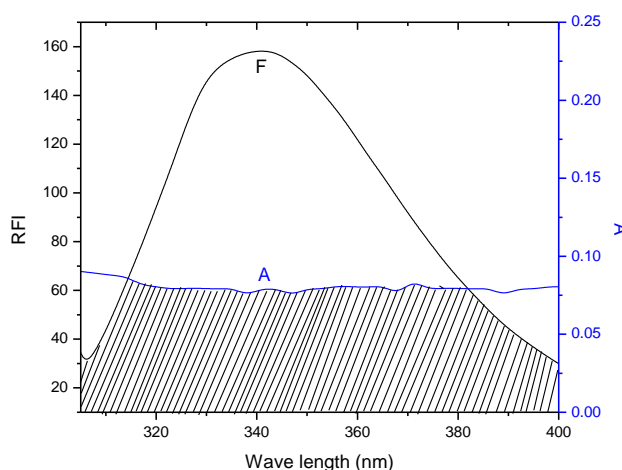

Fig. 8. Spectral overlap of Ag-PVT nanoparticles absorption (curve A) with fluorescence of BSA (curve F). Concentration of BSA and Ag-PVT were 1.5 µM and 24 µM, respectively.

$$E = 1 - \frac{F}{F^0} = \frac{R_0^6}{R_0^6 - r^6} \tag{7}$$

where r is the distance between acceptor (Ag-PVT nanoparticle) and donor (BSA) and R_0 is the critical distance when the transfer efficiency is 50%. The value for R_0 is calculated using Eqs. (7) and (8): [53]

$$R_0^6 = 8.8 \times 10^{-25} k^2 N^{-4} \Phi J \tag{8}$$

where N is the refractive index of the medium, k^2 is the orientation factor, and Φ is the quantum yield of the donor. The spectral overlap integral (J) between the donor emission spectrum and the acceptor absorbance spectrum was approximated by the following summation

$$J = \frac{\sum F(\lambda)\varepsilon(\lambda)\lambda^4 \Delta\lambda}{\sum F(\lambda)\Delta\lambda} \tag{9}$$

where $F(\lambda)$ and $\varepsilon(\lambda)$ represent the fluorescence intensity of the donor and the molar extinction coefficient of the acceptor, respectively. From these relationships J, E and R_0 can be calculated. For the BSA-ligand interaction, $K^2 = 2/3$, N=1.336 and $\Phi = 0.15$ [40]. According to the above equations following values of the parameters were obtained: J = 4.8 x 10^{-15} cm^{3}Lmol^{-1}, R_0 = 2.16 nm, E =0.165 and r =2.84 nm. As the donor–to-acceptor distance for the BSA–Ag-PVT system is less than 8 nm and $0.5 R_0 < r < 1.5 R_0$, which implies high probability of energy transfer from BSA to Ag-PVT nanoparticles. Besides, the donor-to-acceptor distance is less than 8 nm, indicating again that the static quenching interaction occurred between BSA and Ag-PVT nanoparticles.

4. Conclusions

Modification of silver nanoparticles was undergone using polyvinylthiol as stabilizing agent. Interaction of these nanoparticles (AG-PVT) with bovine serum albumin (BSA) was investigated exploiting UV-visible, florescence (intrinsic, extrinsic and synchronous) and circular dichroism spectroscopic techniques. The quenching of BSA fluorescence takes place with 1:1 complex formation between the albumin and nanoparticle. Hydrophobic forces play significant role in the conformational changes during the binding process and BSA gets partially unfolded in presence of Ag-PVT nanoparticles. The quenching process was found to be static with a binding distance of 2.84 nm between the BSA and nanoparticle.

Acknowledgement

References

[1] F. Watari, N. Takashi, A. Yokoyama, M. Uo, M. Akasaka, Y. Sato, S. Abe, Y. Totsuka, K. Tohji, J. Roy. Soc. Interface **6**, S371 (2009).
[2] C. Fillafer, D. S. Friedl, A. K. Ilyes, M. Wirth, F. Gabor, J. Nanosci. Nanotechnol. **9**, 3239 (2009).
[3] X. Gao, Y. Cui, M. Levenson, L. W. K. Chung, S. Nie, Nat. Biotechnol. **22**, 969 (2004).
[4] M. De, P. S. Ghosh, V. M. Rotello, Adv. Mater. **20**, 4225 (2008).

[5] N. Saito, H. Haneda, N. Sekiguchi, I. Ohashi, K. Sekiguchi, K. Kaumoto, Adv. Mater. **14**, 418 (2002).

[6] A. E. Welles, Silver Nanoparticles: Properties, Characterization and Applications: Nanotechnology science and technology series, Nova Science Publishers Inc., New York (2010).

[7] S. Sivolella, E. Stellini, G. Brunello, C. Gardin, L. Ferroni, E. Bressan, B. Zavan, J. Nanomaterials 975842 (2012).

[8] R. Garcıa-Contreras, L. Argueta-Figueroa, C. Mejia-Rubalcava, R. Jimenez-Martinez, S. Cuevas-Guajardo, P. A. Sanchez- Reyna, H. Mendieta-Zeron, Int. Dental J. **61**, 297 (2011).

[9] M.K. Rai, S.D. Deshmukh, A.P. Ingle and A.K. Gade, J. Appl. Microbiol. **112**, 841(2012).

[10] E. Ruckenstein, Z.F. Li, Adv. Colloid Interface Sci. **113**, 43 (2005).

[11] V. Labhasetwar, D.L. Leslie-Pelecky, Biomedical Applications of Nanotechnology, John Wiley & Sons Inc., Hoboken, NJ (2007).

[12] S. Jiang, K. Y. Win, S. Liu, C. P. Teng, Y. Zheng, M.-Y. Han, Nanoscale, **5**, 3127 (2013).

[13] N. M. Bahadur, T. Furusawa, M. Sato, F. Kurayama, I. A. Siddiquey, N. Suzuki, J Colloid Interface Sci. **355**, 312 (2011).

[14] K. Kim, H. B. Lee, J. W. Lee, K. S. Shin, J Colloid Interface Sci. **345**, 103 (2010).

[15] Y. Tan, Y. Wang, L. Jiang, D. Zhu, J Colloid Interface Sci. **249**, 336 (2002).

[16] P. He, X. Zhu, Mater. Res. Bull. **43**, 625 (2008).

[17] A. Stewart, S. Zheng, M. R. McCourt, S. E. J. Bell, ACS Nano **6**, 3718 (2012).

[18] S. Bhat, U. Maitra, J. Chem. Sci., **120**, 507 (2008).

[19] W. Gan, B. Xu, H.-L. Dai, Angew. Chem. Int. Ed. **50**, 6622 (2011).

[20] C. A. Bauer, F. Stellacci, J. W. Perry, Top. Catal. **47**, 32 (2008).

[21] C. Battocchio, C. Meneghini, I. Fratoddi, I. Venditti, M. V. Russo, G. Aquilanti, C. Maurizio, F. Bondino, R. Matassa, M. Rossi, S. Mobilio, G. Polzonetti, J. Phys. Chem. C **116**, 19571 (2012).

[22] A. Andrieux-Ledier, B. Tremblay, A. Courty, Langmuir **29**, 13140 (2013).

[23] H. Yang, Y. Wang, H. Huang, L. Gell, L. Lehtovaara, S. Malola, H. Hakkinen, N. Zheng, Nature Commun. **4**, 2422 (2013).

[24] A. M. Atta, H. A. Al-Lohedan, A. O. Ezzat, Molecules **19**, 6737 (2014).

[25] X.M. He, D.C. Carter, Atomic structure and chemistry of human serum albumin, Nature **358**, 209 (1992).

[26] T. Peters Adv. Protein Chem. **37**, 161 (1985).

[27] P. Joshi, S. Chakraborty, S. Dey, V. Shanker, Z.A. Ansari, S.P. Singh, P Chakrabarti, J. Colloid Interface Sci. **355**, 402 (2011).

[28] A. Gebregeorgis, C. Bhan, O. Wilson, D. Raghavan, , J. Colloid Interface Sci. **389**, 31 (2013).

[29] T. Winuprasith, M. Suphantharika, D.J. McClements, L. He, J. Colloid Interface Sci. **416**, 184 (2014).

[30] J. Saikia, B. Saha, G. Das, J. Colloid Interface Sci. **416**, 235 (2014).

[31] C. Bhan, T.L. Brower, D. Raghavan, , J. Colloid Interface Sci. **402**, 40 (2013).

[32] A. Bhogalea, N. Patel, J. Mariam, P.M. Dongre, A. Miotello, D.C. Kothari, Colloids Surf. B: Biointerfaces **113**, 276 (2014).

[33] M. S. Ali, H. A. Al-Lohedan, M.Z.A. Rafiquee, A. M. Atta, A. O. Ezzat, Spectrochim. Acta A: Mol. Biomol. Spectr. **135**, 147 (2014).

[34] L. JR, Principles of Fluorescence Spectroscopy, Springer, New York 3rd edition (1999).

[35] U. Anand, C. Jash, S. Mukherjee, J. Phys. Chem. B **114**, 15839 (2010).

[36] X.Z. Feng, Z. Lin, L.J. Yang, C. Wang, C.L. Bai, Talanta **47**, 1223 (1998).

[37] W.C. Johnson, Jr., Proteins **7**, 205 (1990).

[38] Y.H. Chen, J.T. Yang, H.M. Martinez, Biochemistry **11**, 4120 (1972).

[39] C. Louis-Jeune, M.A. Andrade-Navarro, C. Perez-Iratxeta, Proteins Struct. Func. Bioinfo. **80**, 374 (2012).

[40] M.S. Ali, H.A. Al-Lohedan, Mol. Biol. Rep. **40**, 6081 (2013).

[41] M.S. Ali, H.A. Al-Lohedan, J. Mol. Liq. **197**, 124 (2014).

[42] O.K. Abou-Zeid, O.I.K. Al-Shihi, J. Am. Chem. Soc. **130**, 10793 (2008).

[43] T. Yuan, A.M. Weljie, H.J. Vogel, Biochemistry, **37**, 3187 (1998).

[44] J. Slavik, Biochim. Biophys. Acta **694**, 1 (1982).

[45] D. Sarkar, RSC Adv. **3**, 24389 (2013).

[46] Y.-Q. Wang, H.-M. Zhang, G.-C. Zhang, S.-X. Liu, Q.-H. Zhou, Z.-H. Fei, Z.-T. Liu, Int. J. Biol. Macromol. **41**, 243 (2007).

[47] T. Peters, Jr., All About Albumin: Biochemistry, Genetics, and Medical Applications, Academic Press, London (1995).

[48] S.M. Kelly, T.J. Jess, N.C. Price, Biochim. Biophys. Acta **1751**, 119 (2005).

[49] S.M. Kelly, N.C. Price, **1**, 349 (2000).

[50] M. S. Ali, N. Gull, J. M. Khan, V. K. Aswal, R. H. Khan, Kabir-ud-Din, J. Colloid Interface Sci. **352**, 436 (2010).

[51] J. M. Khan, A. Qadeer, S. K. Chaturvedi, E. Ahmad, S. A. A. Rehman, S. Gourinath, R. H. Khan, Plos One **7**, e29694 (2012).

[52] T. Förster, Delocalized excitation and excitation transfer, in Modern Quantum Chemistry, Vol. 3, O. Sinanoglu (Ed.), Academic Press, New York (1996).

[53] J. Kang, Y. Lu, M.X. Xie, S. Li, M. Jiang, Y.D. Wang, Biochim. Biophys. Acta **1674**, 205 (2004).